



Evaluating global paleoshoreline models for the Cretaceous and Cenozoic

C. HEINE*, L. G. YEO AND R. D. MÜLLER

EarthByte Group, School of Geosciences, Madsen Building F09, The University of Sydney, NSW 2006, Australia.

Paleoshoreline maps represent the distribution of land and sea through geological time. These compilations provide excellent proxies for evaluating the contributions non-tectonic vertical crustal motions, such as mantle convection-driven dynamic topography, to the flooding histories of continental platforms. Until now, such data have not been available as a globally coherent compilation. Here, we present and evaluate a set of Cretaceous and Cenozoic global shoreline data extracted from two independent published global paleogeographic atlases. We evaluate computed flooding extents derived from the global paleoshoreline models with paleo-environment interpretations from fossils and geological outcrops and compare flooding trends with published eustatic sea-level curves.

Although the implied global flooding histories of the two models are similar in the Cenozoic, they differ more substantially in the Cretaceous. This increase in consistency between paleoshoreline maps with the fossil record from the Cretaceous to the Cenozoic likely reflects the increase in the fossil preservation potential in younger geological times. Comparisons between the two models and the Paleogeographic Atlas of Australia on a regional scale in Australia reveal a higher consistency with fossil data for one model over the others in the mid-Cretaceous and suggest that a review of the interpretation of the Late Cretaceous–Cenozoic paleogeography may be necessary. The paleoshoreline maps and associated paleobiology data constraining marine vs terrestrial environments are provided freely as reconstructable GPlates-compatible digital files and form a basis for evaluating the output of geodynamic models predicting regional dynamic surface topography.

KEY WORDS: paleogeography, paleoshorelines, fossils, lithology, database, evaluation.

INTRODUCTION

Paleogeographic maps of the Earth depict the evolution of land and sea through geological time. These interpretations of the geological record, along with plate reconstructions, allow the construction of time-dependent paleo-environmental distributions (e.g. Hay *et al.* 1999; Blakey 2003). The boundary between terrestrial and marine paleo-environments is marked by paleoshoreline locations. Lateral displacements between paleoshoreline locations through time serve as indicators of vertical motions (e.g. Veevers & Morgan 2000; Heine *et al.* 2010), which may be linked to mantle convection and eustasy (e.g. Gurnis 1990, 1993; Gurnis *et al.* 1998; Heine *et al.* 2010; Spasojevic & Gurnis 2012).

However, only a few global paleogeographic compilations (e.g. Ronov *et al.* 1989; Smith *et al.* 1994; Scotese 2004; Golonka *et al.* 2006; Blakey 2008), which adequately sample the geological history at sampling intervals of 5–15 million years and which have been build based on relatively recent plate kinematic models, are publicly accessible. Most of these compilations are not associated with georeferenced, digital data, and the original references for local paleo-environment interpretations are difficult to trace. These atlases, however, contain

valuable syntheses of paleo-environment interpretations from seismic, well and outcrop data, commonly also supported by proprietary exploration industry data. The highly derivative and limited traceable origins of local paleo-environment interpretations in large-scale paleogeographic maps, necessitate independent verification with other data, such as surface lithological outcrop data and interpreted paleo-environments from fossils.

Here, we evaluate Cretaceous and Cenozoic paleoshorelines from two independent global paleogeographic atlases (Smith *et al.* 1994; Golonka *et al.* 2006). First, we derive the global flooding history from both compilations and compare it with eustatic sea-level curves. We further compare the extents of flooding with fossil-derived paleo-environment interpretations from the Fossilworks (formerly PaleoDB) database (<http://www.fossilworks.org>). These analyses are repeated on a regional scale in Australia for the aforementioned paleoshoreline models and the Paleogeographic Atlas of Australia (Langford *et al.* 1995).

PALEOGEOGRAPHIC ATLASES USED IN THIS STUDY

Two global paleogeographic atlases (Smith *et al.* 1994; Golonka *et al.* 2006) were used to extract paleoshoreline

*Corresponding author: christian.heine@shell.com

Table 1 Nominal ages of Golonka *et al.* (2006)'s maps and their numerical equivalents as defined by Sloss (1988) and Gradstein *et al.* (2004).

Nominal age	Numerical age			
	Sloss (1988)		Gradstein <i>et al.</i> (2004)	
	Start age (Ma)	End age (Ma)	Start age (Ma)	End age (Ma)
Upper Tejas III	11.0	2.0	12.8	1.8
Upper Tejas II	20.0	11.0	22.3	12.8
Upper Tejas I	29.0	20.0	30.5	22.3
Lower Tejas III	37.0	29.0	36.6	30.5
Lower Tejas II	49.0	37.0	48.6	36.6
Lower Tejas I	58.0	49.0	58.4	48.6
Upper Zuni IV	81.0	58.0	83.8	58.4
Upper Zuni III	94.0	81.0	98.0	83.8
Upper Zuni II	117.0	94.0	123.0	98.0
Upper Zuni I	135.0	117.0	139.0	123.0
Lower Zuni III	146.0	135.0	147.8	139.0

locations. The global paleogeographic map compilation of Golonka *et al.* (2006) spans the Phanerozoic and is subdivided into 32 time-steps based on the Sloss (1988) time-scale (see Table 1; Figure 1). These time-steps are bound by stratigraphic unconformities (e.g. the 94–81 Ma interval starts at the middle Cenomanian unconformity and ends at the lower Campanian unconformity). The Smith *et al.* (1994) compilation covers the Mesozoic and Cenozoic in 31 time-steps, defined by stage boundaries (e.g. Berriasian to Valanginian; Maastrichtian), and assigns numerical age ranges based on the Harland (1990) time-scale (see Table 2; Figure 1). In the Cretaceous and Cenozoic, the Golonka *et al.* (2006) maps are integrated over longer time intervals compared with the Smith *et al.* (1994) maps (Figure 1; Tables 1, 2). For example, Golonka *et al.* (2006)'s Upper Zuni III interval (98–83.8 Ma after Gradstein *et al.* 2004) comprises two intervals of Smith *et al.* (1994)'s maps (93.5–89.3 Ma and 89.3–85.8 Ma following the time-scale of Gradstein *et al.* 2004).

The Golonka *et al.* (2006) paleogeographic classification groups data into ice sheet, landmass, highland, shallow sea, continental slope, and deep ocean basin paleoenvironments. In contrast, Smith *et al.* (1994)'s classification is ternary, delineating the onshore/offshore boundaries through paleoshoreline locations, and a further

onshore subdivision into 'areas of higher relief' based on data from the Paleogeographic Atlas Project (PGAP, <http://www.geo.arizona.edu/~rees/PGAPhome.html>). In both atlases, no paleo-elevation data were tied to the different paleo-environments, allowing only paleoshorelines to be quantitatively compared against each other. In frontier, less sampled parts of the world, the atlases infer that 'reasonable' estimates of paleoshorelines were interpolated from adjacent time-steps. Such interpolations assumed, for example, that Antarctica was elevated for most of the Mesozoic and Cenozoic except where marine deposits were known to be present (Smith *et al.* 1994).

Paleo-environment distributions from Smith *et al.* (1994) and Golonka *et al.* (2006) were synthesised from global and regional paleogeography papers, as well as proprietary datasets; Smith *et al.* (1994) does not list source references published after 1985. As many of the sources were collected in the 'pre-digital' era, clear detail on data coverage, spatial accuracy and interpolation methods is impossible to retrace. The paleo-environment interpretations were compiled from various data sources including surface rock outcrops, (proprietary) well- and seismic-reflection data, fossils, as well as earlier published global paleogeographic maps (e.g. Veevers 1969;

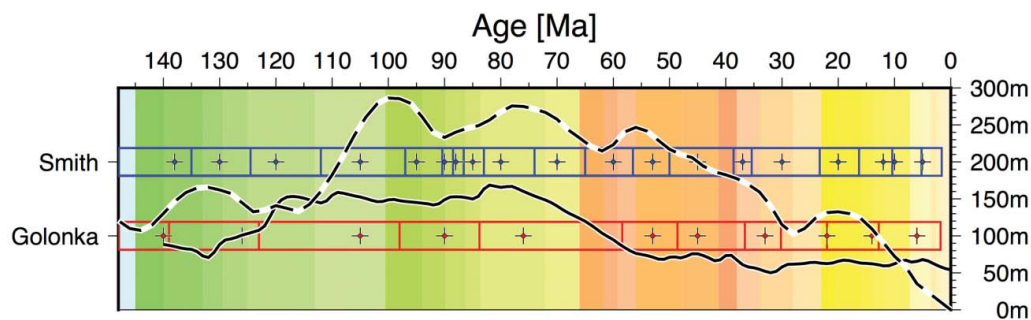


Figure 1 Overview of the time intervals (rectangles) and reconstruction ages (crosses) for the two global paleogeographic atlas projects. Golonka *et al.* (2006): red and Smith *et al.* (1994): blue. Background colours correspond to geological stages from the GTS 2004 time-scale (<http://bitbucket.org/chhei/gmt-cpts>). Right side of plot shows eustatic sea-level estimates of Haq & Al-Qahtani (2005, filtered, 10 Ma moving window as dashed black line) and Müller *et al.* (2008, as solid black line).

Table 2 Nominal ages of Smith *et al.* (1994)'s maps and their numerical equivalents as defined by Harland (1990) and Gradstein *et al.* (2004).

Nominal age	Numerical age			
	Harland (1990)		Gradstein <i>et al.</i> (2004)	
	Start age (Ma)	End age (Ma)	Start age (Ma)	End age (Ma)
Pliocene	5.2	1.6	5.3	1.8
Late Miocene	10.4	5.2	11.6	5.3
Middle Miocene	16.3	10.4	16.0	11.6
Early Miocene	23.3	16.3	23.0	16.0
Oligocene	35.4	23.3	33.9	23.0
Late Eocene	38.6	35.4	37.2	33.9
Middle Eocene	50.0	38.6	48.6	37.2
Early Eocene	56.5	50.0	55.8	48.6
Paleocene	65.0	56.5	65.5	55.8
Maastrichtian	74.0	65.0	70.6	65.5
Campanian	83.0	74.0	83.5	70.6
Santonian	86.6	83.0	85.8	83.5
Coniacian	88.5	86.6	89.3	85.8
Turonian	90.4	88.5	93.5	89.3
Cenomanian	97.0	90.4	99.6	93.5
Albian	112.0	97.0	112.0	99.6
Aptian	124.5	112.0	125.0	112.0
Barremian–Hauterivian	135.0	124.5	136.4	125.0
Valanginian–Berrisian	145.6	135.0	145.5	136.4

Petters 1979; Masson & Roberts 1981; Hahn 1982; Blakey & Gubitosa 1984; Ronov *et al.* 1989; Winterer 1991; Kiessling *et al.* 1999, 2003; Kiessling & Flügel 2000). Unpublished paleo-environment datasets were also integrated into the Golonka *et al.* (2006) global paleogeographic maps from the PALEOMAP group (University of Texas at Arlington), the PLATES project (University of Texas at Austin), the PGAP group at the University of Chicago, the Institute of Tectonics of Lithospheric Plates in Moscow, Robertson Research in Llandudno (Wales) and the Cambridge Arctic Shelf Programme (CASP). For Australian paleogeography, Golonka *et al.* (2006) cites maps from the Paleogeographic Atlas of Australia as their source (BMR Paleogeographic Group 1990).

In both compilations, mapped and interpreted paleo-environment data were rotated back to their paleopositions for the corresponding time intervals using different plate kinematic models and software. The final publications show only the reconstructed paleogeographic maps and hence require a reverse engineering of both plate/terrane outlines as well as the plate motion models. In each case, the plate motion models as well as the corresponding plate/terrane outlines are either not available or incomplete (e.g. missing references). Both compilations are based on different absolute geological time-scales.

Smith *et al.* (1994)'s reconstructions were generated by BP's proprietary software using plate rotations primarily based on ocean-floor magnetic anomaly records from the Atlantic and Indian oceans (see references in Smith *et al.* 1994). For the publication, the paleoshoreline locations in their original present-day positions were transferred to the ATLAS plate reconstruction software

(Cambridge Paleomap Services 1993) and were back-rotated to their paleopositions again using new rotations to generate the published maps. These new rotations are not provided in Smith *et al.* (1994). We compiled the plate-rotation data from their references list, which revealed differences between the rotation poles in the listed references and the new rotations used to generate the final maps.

REVERSE ENGINEERING OF PALEOSHORELINE DATA

We extracted paleoshorelines from the Smith *et al.* (1994) and Golonka *et al.* (2006) and maps covering the past 150 Ma. Jan Golonka kindly provided digital copies of global reconstruction maps in Corel Draw® vectorgraphics format. These were turned into AutoCAD® files and georeferenced in ESRI's ArcGIS®. For Smith *et al.* (1994), we scanned the map paper copies and subsequently georeferenced and digitised the images. Once the data were available in ESRI Shapefile format, we rotated them to their present-day positions using the interactive open-source plate reconstruction software GPlates (Boyden *et al.* 2011, <http://www.gplates.org/>).

Tables 1 and 2 list the numerical stratigraphic age intervals of the two paleogeographic atlases in their original time-scales and the equivalent converted ages based on Gradstein *et al.* (2004). Given the incomplete plate motion histories and uncertainties of the origin of local paleo-environment interpretations in both compilations, the resultant paleoshoreline locations are subject to plate rotation and paleogeographic interpretation errors that are not quantifiable. We attempt to address

this issue by comparing the paleoshoreline locations with independent datasets. It should be noted that the paleogeography of Antarctica as represented in both atlases is not addressed in this paper.

The first step in comparing the two paleoshoreline models was to assess the similarity of predicted inundation of the continental areas from both models over the past 150 Ma. Here we use the present-day total area of continental crust ($2.22 \times 10^8 \text{ km}^2$) as a base for our computations. This estimate includes the extent of continental crust as defined by boundaries between continental and oceanic crust. For both atlases and for each reconstruction time interval, we compute the area of land relative to the total area of continental crust at present day as well as against two eustatic sea-level estimates (Haq & Al-Qahtani 2005; Müller *et al.* 2008). As we are only interested in the long-term sea-level trend, the global sea-level curve of Haq & Al-Qahtani (2005) was filtered using a cosine arch filter within a 10 Myr moving window to isolate long-wavelength components.

Both paleoshoreline estimates, with interpreted paleoenvironments from the Paleobiology database, were compared by extracting 'marine' and 'terrestrial' fossil locations corresponding to each key reconstruction time step. Here, the number of terrestrial or marine fossils from the collection contained within land or marine paleogeographic extents, respectively, at each reconstruction time

interval in each atlas is taken as the measure of paleoshoreline–fossil consistency (Figure 2).

The time-dependent changes, between paleoshoreline locations of selected time-steps in both paleogeographic atlases, produce patterns of regression and transgression in certain areas. Here, we evaluate the lateral paleoshoreline changes in the intervals 140–126 Ma, 105–90 Ma, 105–76 Ma and 76–6 Ma for Golonka *et al.* (2006), and 130–120 Ma, 105–70 Ma and 60–5 Ma for Smith *et al.* (1994).

FLOODING HISTORIES

The time-dependent changes in global land area computed from both paleogeographic atlases for the Cretaceous and Cenozoic reconstructions show a progressive increase in land area towards the present, with a phase major shoreline advancement towards the continents correlating with the Cretaceous sea-level highstand between 120 and 70 Ma (Figure 3). Similarities in the predicted amount of land area exist between the Smith *et al.* (1994) and Golonka *et al.* (2006) atlases at around 140 Ma, between 120 and 105 Ma and throughout the Cenozoic. As expected, long-wavelength patterns of global sea-level variations (*ca* 30 Ma) correlate well with the flooding histories of both paleoshoreline models.

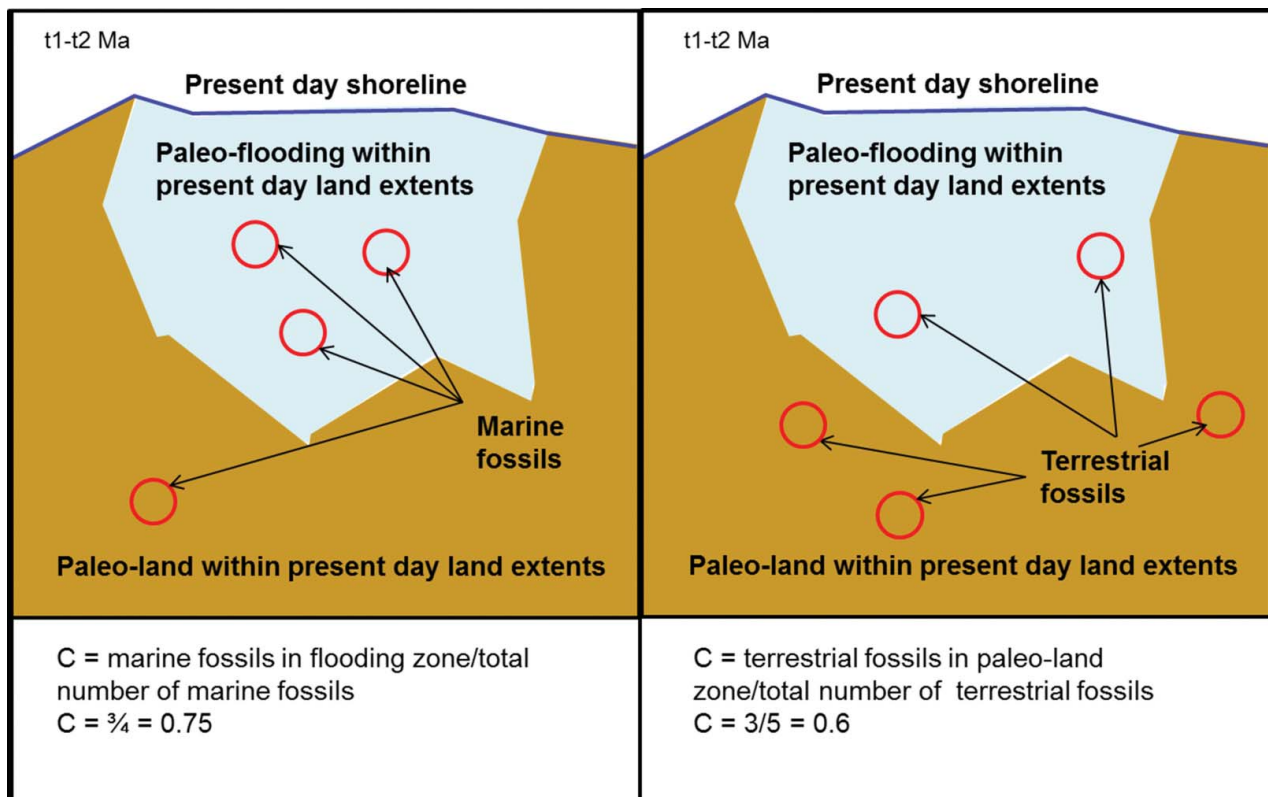


Figure 2 Conceptual diagram of consistency evaluations of fossils with paleoshoreline locations. The present-day shoreline is shown as a blue line. For time t1–t2 Ma flooding and land extents are shown in cyan and orange, while fossil locations as shown as red circles. Left: marine fossil locations within flooded areas at time t1–t2 Ma within present-day land extents are taken to be a measure of paleoshoreline–fossil consistency as shown by the equation at bottom left. Right: terrestrial fossil locations within paleoland areas at time t1–t2 Ma are taken to be a measure of paleoshoreline–fossil location consistency as shown by the equation at bottom right.

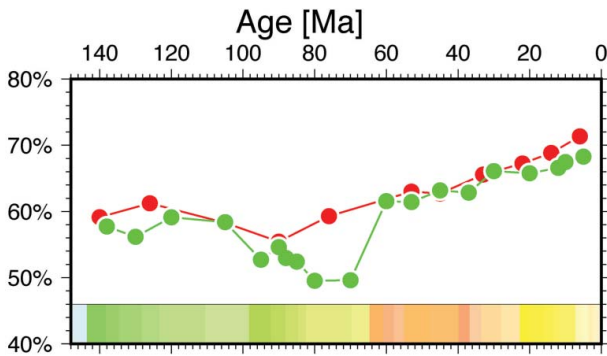


Figure 3 Inundation history of continental ‘land’ area relative to total area of present-day continental crust as implied by the two paleogeographic atlases (red: Golonka *et al.* 2006; green: Smith *et al.* 1994). Larger values indicate less flooding (larger exposed continental area relative to total area of continental crust). Note the progressive increase in exposed land area during the Cenozoic and the relative consistency between the two paleogeographic atlases.

Smith *et al.* (1994) indicates greater flooding compared with Golonka *et al.* (2006) in the earliest Early Cretaceous and throughout the mid- to Late Cretaceous. These time intervals generally correlate with a higher ‘sampling rate’ of the Smith *et al.* (1994) model in comparison with Golonka *et al.* (2006) of about 2:1. In Australia, the flooding histories of both models qualitatively match the patterns extracted from Langford *et al.* (1995; Figure 4). The Australian sea-level fall predicted by these models, however, has a minor offset against the regional paleogeographic compilations that we attribute to differences in time-scales used for the atlases. Further, the relatively large inundation of Australia during this time contrasts with the mid-Cretaceous global sea-level highstand (Figure 1). This mismatch is attributed to mantle convection-induced negative dynamic topography during this time (Matthews *et al.* 2011; Spasojevic & Gurnis 2012).

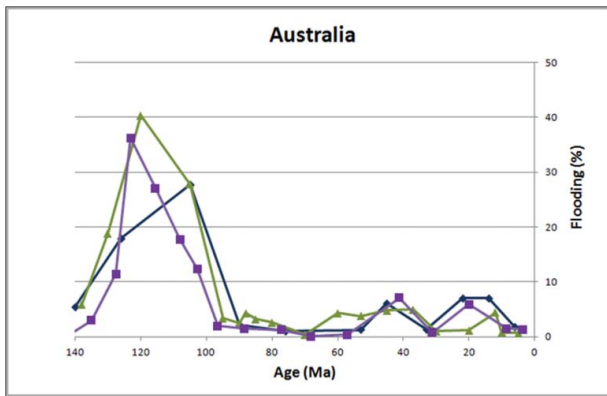


Figure 4 Australian flooding histories derived from Golonka *et al.* (2006) (in dark blue), Smith *et al.* (1994) (in olive green) and Langford *et al.* (1995) (in purple) expressed as percentage age relative to the present-day land extent.

FOSSIL AND FLOODING DISTRIBUTIONS

For the Early Cretaceous time intervals, predominant fossil locations cluster in East Asia, Central Asia, north-eastern India, mainland Europe, northern Africa, eastern Australia and the western half of the Americas (Figures 5, 6). The interpreted inundation in the Early Cretaceous (138 Ma) of Smith *et al.* (1994) relative to the less extensive 140 Ma flooding interpreted by Golonka *et al.* (2006) (cf. Figure 3) is mainly caused by differences in estimated flooding extents in regions that have subsequently undergone a complex tectonic history, such as in northeast India, Southeast Asia and Alaska, but differences also exist along the northwestern African margin (Figure 5). Marine fossil distributions support Smith *et al.* (1994)’s greater flooding extents at 138 Ma. For the 130 Ma time slice, Smith *et al.* (1994) show more extensive transgression in the West Siberian Basin area, and northern Africa, whereas Golonka *et al.* (2006)’s 126 Ma paleoshorelines show a greater extent of flooding across the Western Interior seaway in North America (Bond 1976; Figure 6). However, this is not supported by the distribution of fossils (Figure 6, top).

The distribution patterns of marine fossil records show further prominent disagreements for Smith *et al.* (1994) and Golonka *et al.* (2006) for locations in southeast Asia where both models predict no flooding in areas of recorded marine fossils (Figure 6). Marine fossils indicate that the epicontinental sea in eastern Australia should be larger in extent compared with the Smith *et al.* (1994) and Golonka *et al.* (2006) interpretations (Figure 6).

We have also compared whether resulting transgression/regression patterns for both paleoshoreline models match the fossil record for 3 distinct time intervals. Estimated flooding patterns for the time intervals 140–126 Ma (Golonka *et al.* 2006) and 138–120 Ma (Smith *et al.* 1994) show again discrepancies in areas of post-Jurassic tectonic complexity such as the Himalayas and the Mediterranean region where the models indicate regression in contradiction to marine fossil records from this time slice (Figure 7). In Iran and eastern Arabia, and along the future Western Interior Seaway in Northern America, Golonka *et al.* (2006)’s paleocoastlines infer progressive transgression, contradicting published paleogeographic estimates (Ziegler 2001) and fossil records, respectively (Figure 7, top panel). Smith *et al.* (1994)’s flooding patterns indicate a vast transgression across Central Australia, which is not supported by fossil data (Figure 7, lower panel). For the mid-Cretaceous time slice (105–76/70 Ma; Figure 8), Golonka *et al.* (2006)’s flooding patterns do largely match patterns recorded by land and marine fossil distributions with a notable exception being the various marine incursions across Central Africa (Figure 8, top and middle panel). According to the Smith *et al.* (1994) compilation, vast inland tracts of central North America are flooded; however, this is not supported by marine fossil occurrences for the equivalent time slice. Major differences exist between both models for the flooding patterns in North America, across northern Africa and in the Middle East–Caspian–Volga–West Siberian Basin region. In Australia, the continent-wide regression of

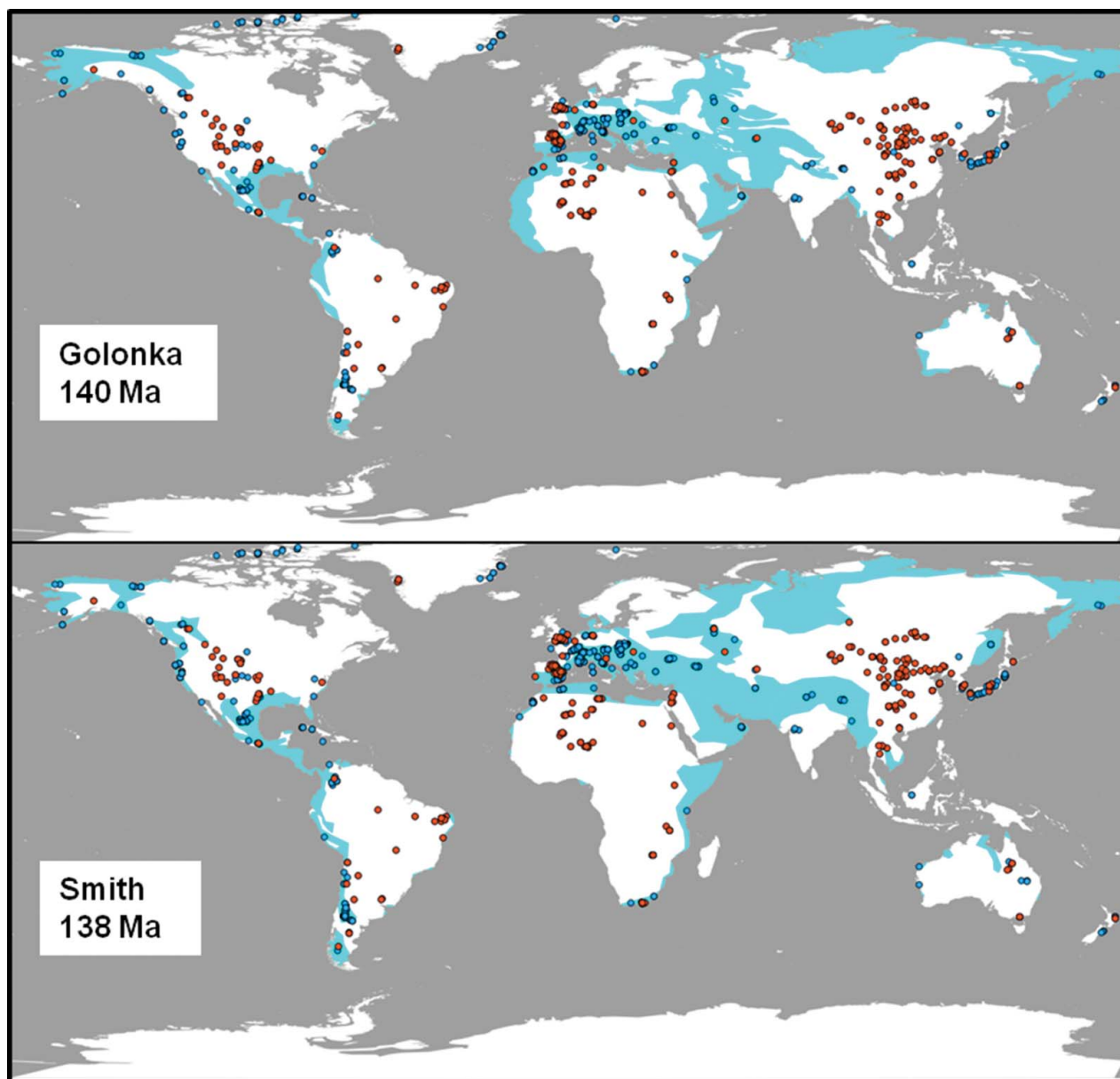


Figure 5 Present-day land extents (white) that were flooded at 140 Ma (Golonka *et al.* 2006) and 138 Ma (Smith *et al.* 1994), marked in cyan. Terrestrial fossil locations are marked as dark orange circles and marine fossil locations are marked as blue circles.

the Early Cretaceous seaway is supported by regional models (Langford *et al.* 1995) and some fossil records (Figure 8).

The consistency of both paleoshoreline models with fossil records over the past 140 Ma has changed considerably (Figure 9). Marine fossil–paleoshoreline consistency ratios range between ~30% and ~75% for the past 140 Ma for both models. While the ratios for the Golonka *et al.* (2006) model vary over a narrower band, the ratios for the Smith *et al.* (1994) paleoshoreline models decrease towards the Aptian (~45%) and increase significantly towards the mid Cretaceous (around 75%) before dropping again towards the present (~30%). The overall trends between both models are largely similar. However, a major difference exists in the Early Cretaceous

(126/120 Ma) where Golonka *et al.* (2006)'s fossil–paleoshoreline consistency is larger than that of Smith *et al.* (1994) and during the mid Cretaceous where the values computed for the Smith *et al.* (1994) model are consistently higher than those for Golonka *et al.* (2006). The consistency of the paleoshoreline models with terrestrial fossil occurrences is in general much higher (>40%) for the past 140 Ma for both models (Figure 9, red lines). Here, computed ratios for both models are low during the mid Cretaceous, largely explained by the mismatches in the area of the Western Interior seaway and in the European region (cf. Figure 8).

Cretaceous–Cenozoic Australian land patterns in Smith *et al.* (1994), Golonka *et al.* (2006) and the Paleogeographic Atlas of Australia (Langford *et al.* 1995; Yeung

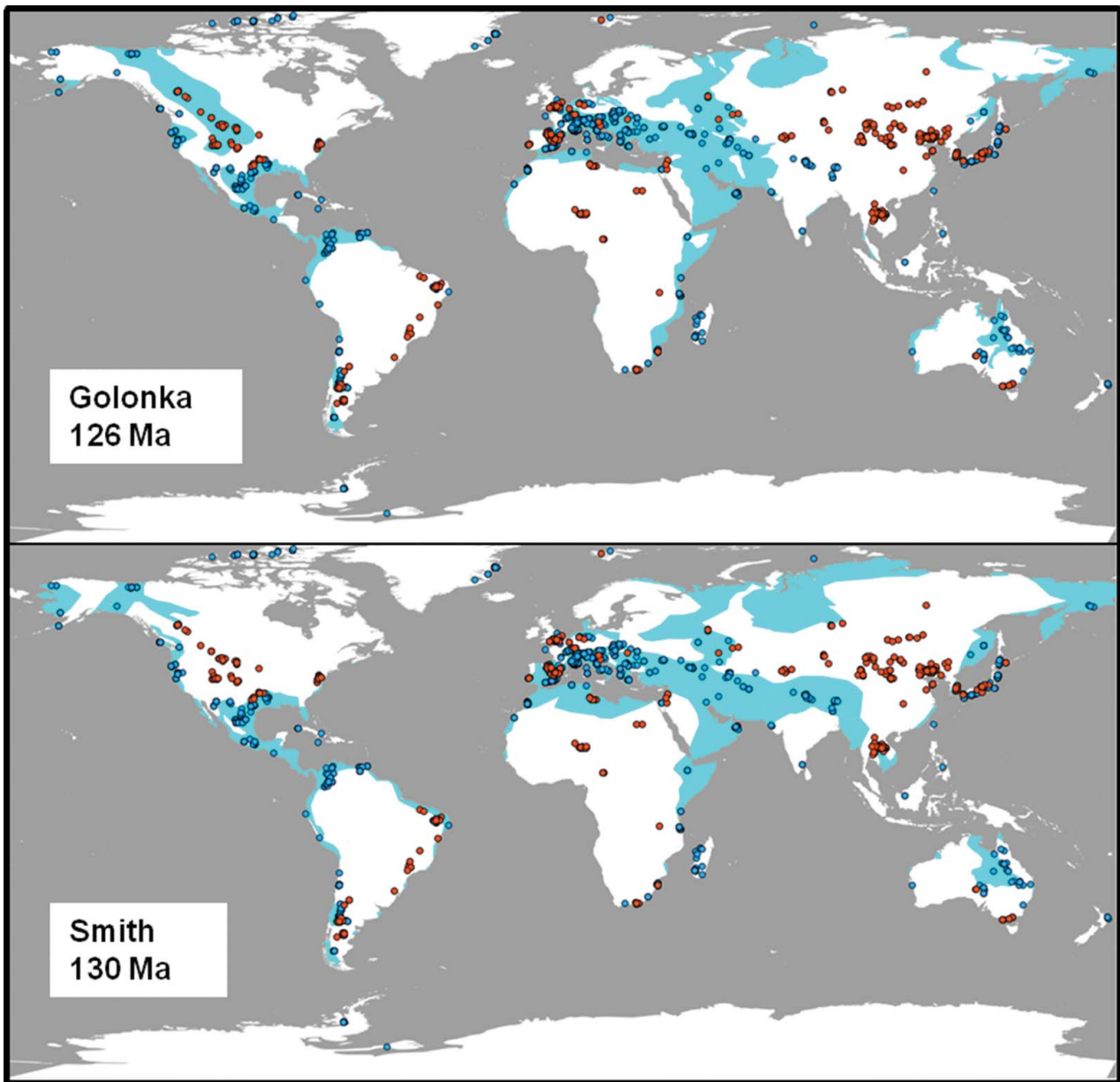


Figure 6 Present-day land extents that were flooded at 126 Ma (Golonka *et al.* 2006) and 130 Ma (Smith *et al.* 1994), marked in cyan. Terrestrial fossil locations are marked as dark orange circles and marine fossil locations are marked as blue circles.

2002) are mostly 100% consistent with terrestrial fossil locations except for a notable drop to a minimum of 50% consistency in the later half of the Late Cretaceous (see Figure 10). The consistency trends between flooding extents and marine fossil locations are more variable for all models.

In the Cretaceous and Cenozoic, the overall consistency of the paleogeographic models with fossil data and minor variations between the models impact on their utility for future studies. The paleoshoreline–fossil consistency trends of the Paleogeographic Atlas of Australia (Langford *et al.* 1995) better matches the patterns of Smith *et al.* (1994) compared with Golonka *et al.* (2006). We attribute this to the differences in chosen time-steps, with

Langford *et al.* (1995) relatively synchronous with Smith *et al.* (1994) but not with Golonka *et al.* (2006). In all mid-Cretaceous paleogeographic reconstruction sets we notice a drop in terrestrial fossil–paleoshoreline consistency compared with earlier times, but this is somewhat less the case for Smith *et al.*'s (1994) maps, which are more consistent with terrestrial fossil locations compared with Golonka *et al.* (2006) and the Paleogeographic Atlas of Australia, owing to their shorter time-steps. Conversely, the Paleogeographic Atlas of Australia is less consistent with marine fossils during the Late Cretaceous–Cenozoic compared with Smith *et al.* (1994) and Golonka *et al.* (2006), also reflecting differences in the length of time-steps. In addition, a Paleogeographic Atlas of Australia

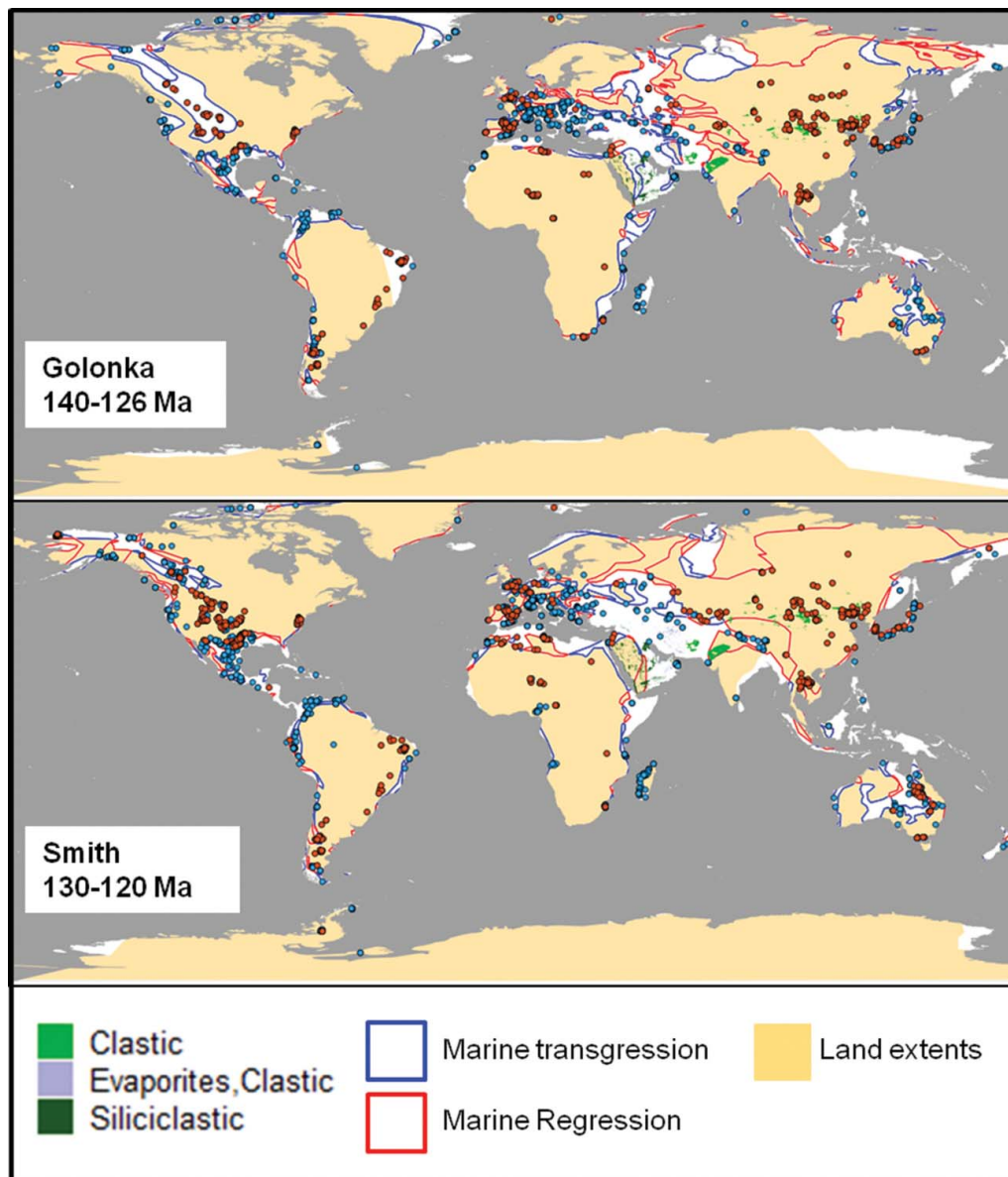


Figure 7 Global maps of marine regression (red outlines) and transgression (blue outlines) patterns with land extents (in light brown) for the Early Cretaceous. Locations of terrestrial and marine fossils are indicated by orange and blue circles, respectively. Classified Early Cretaceous (and younger) sedimentary lithologies (USGS 2011) are also plotted here (see key in Figure 8). Top: 140–126 Ma marine transgression/regression patterns from Golonka *et al.* (2006) with fossil locations and land extents at 126 Ma. Bottom: 130–120 Ma marine transgression/regression patterns from Smith *et al.* (1994) with fossil locations and land extents at 120 Ma.

drop in consistency with terrestrial fossils during the Paleocene–Eocene transition (57 Ma) time step is not present in Smith *et al.* (1994) and Golonka *et al.* (2006).

Synthetic paleoshoreline trajectories

In an attempt to better understand the quality of the paleoshoreline data, we compare the compilation of Smith *et al.* (1994) with horizon interpretations along a seismic reflection profile shot in the Petrel Basin on Australia's northern margin (Figure 11). The seismic line 100/06 of the 1991 'Bonaparte 2' seismic survey covers a wide range of paleoshorelines predicted by the Smith *et al.* (1994) compilation. The

intersections of paleoshorelines and seismic profile should yield information on whether the individual paleoshoreline point falls into a zone in which the seismic interpretation shows a considerable thickness of sediments for the corresponding interpreted stratigraphic package. We used the seismic horizon interpretation from Geoscience Australia (formerly AGSO) to correlate paleoshorelines with subsurface stratigraphy (Colwell & Kennard 2001).

Our synthetic paleoshoreline trajectory plot (Figure 12) highlights where a proposed paleoshoreline position corresponds to a seismic horizon of an adequate thickness that warrants a robust interpretation of seismic facies related to shoreline deposits (such as

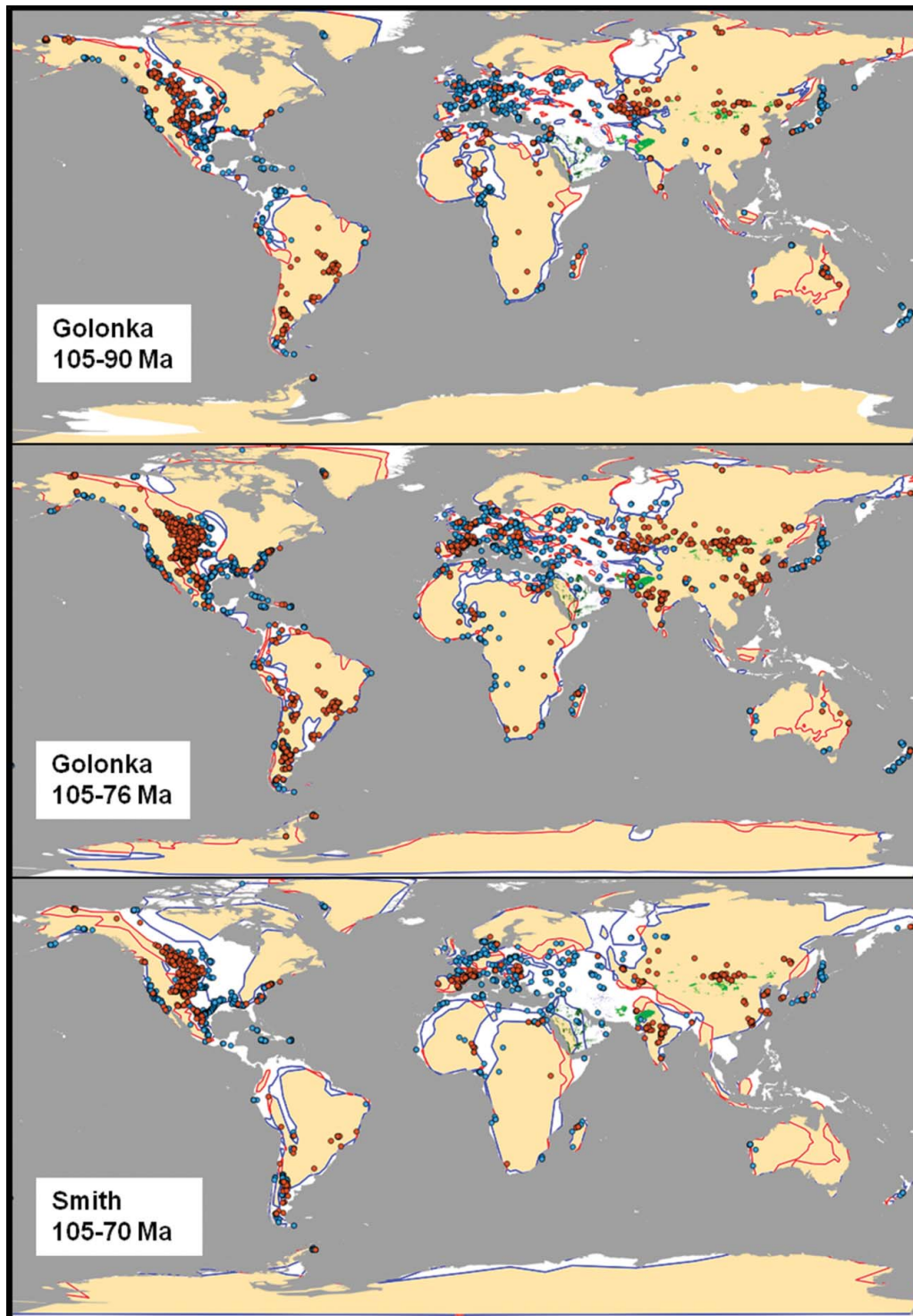


Figure 8 Global maps of marine regression (red outlines) and transgression (blue outlines) patterns with land extents (in light brown) for the mid Cretaceous. Locations of terrestrial and marine fossils are indicated by orange and blue circles, respectively. Classified Late Cretaceous (and younger) USGS (2011) sedimentary lithologies are also plotted here (see key in map). Top: 105–90 Ma marine transgression/regression patterns from Golonka *et al.* (2006) with fossil locations and land extents at 90 Ma. Middle: 105–76 Ma marine transgression/regression patterns from Golonka *et al.* (2006) with fossil locations and land extents at 76 Ma. Bottom: 105–70 Ma marine transgression/regression patterns from Smith *et al.* (1994) with fossil locations and land extents at 70 Ma.

characteristic foresets or beach/delta facies). Absent or thin seismic horizons of a certain age and unconformities highlight geological periods and parts along the section where little or no sediments have been deposited or

eroded and hence place much higher uncertainty on the paleoshoreline position. Time-based trajectories of paleoshoreline locations along the seismic profile allows us to qualitatively constrain the interpretations.

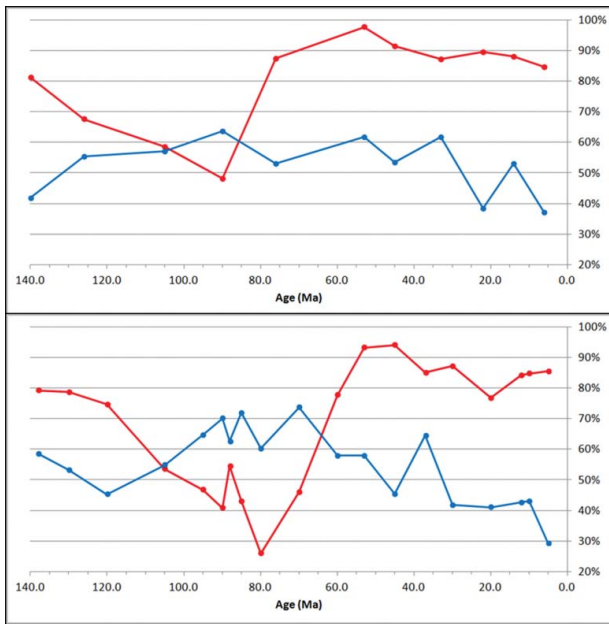


Figure 9 Global consistency ratios, shown as percentages, for the Golonka *et al.* (2006; top) and Smith *et al.* (1994; bottom) paleoshoreline intervals during the Cretaceous and Cenozoic. The consistency curve between land extents and terrestrial fossils is shown as red line, the consistency curve between flooding extents and marine fossils is shown as blue line. The graphs show the ratio of the number of terrestrial/marine fossil locations from the Fossilworks Database corresponding within each land/flooding extent to the total number of terrestrial/marine fossil locations for each time-step. We use the graphs as a proxy for consistency between paleoshorelines interpretations and paleo-environment observations based on fossil data.

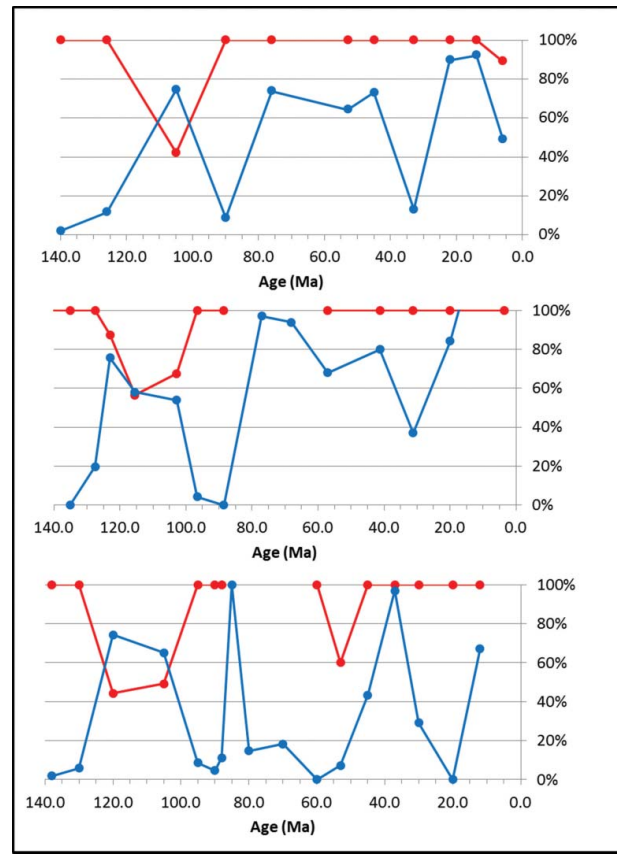


Figure 10 Fossil consistency ratios for the Australian region for the Cretaceous and Cenozoic. Setup as in Figure 7. Comparison of Golonka *et al.* (2006), Smith *et al.* (1994) and Langford *et al.* (1995) with fossil locations from the Fossilworks Database. The consistency curves between land extents and terrestrial fossils are marked in red, while the consistency curve between flooding extents and marine fossils are marked in blue. Top: Golonka *et al.* (2006); middle: Smith *et al.* (1994); bottom: Langford *et al.* (1995). There are no values computed for time-steps without available fossil records.

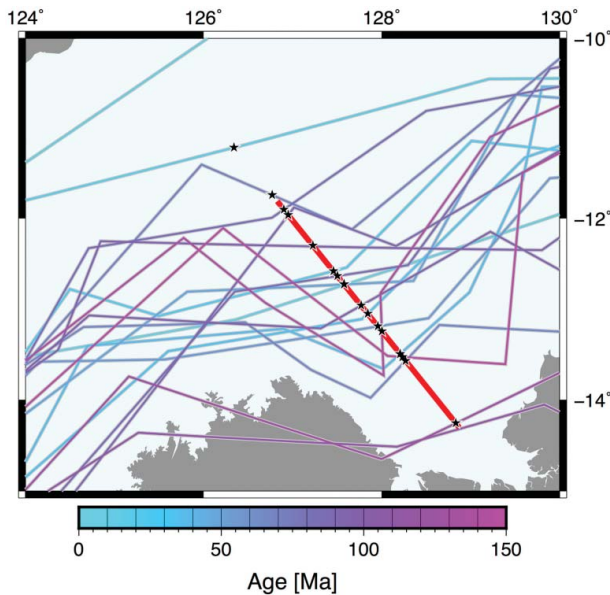


Figure 11 Seismic line AGSO 100/06 location and intersection with Smith *et al.* (1994) paleoshorelines. Thick, red line indicates seismic line location. Coloured solid lines in cool colours are age-coded paleoshorelines from the Smith *et al.* (1994) compilation. Stars indicate intersection points, corresponding to upper plot in Figure 12.

Along profile AGOS 100/06, the Early Cretaceous shoreline intersections, as proposed by the Smith *et al.* (1994) model, correspond to thin and pinching-out horizons of base Cretaceous to Aptian age. Upper Cretaceous shorelines positions place our modelled trajectory within a relatively thick Cenomanian–Turonian to base Cenozoic sequences, which indicate that the shoreline positions are relatively robust and fall within preserved sedimentary packages. Paleocene, mid-Eocene and early Miocene shoreline locations, however, correspond to thin or absent seismic horizons along the profile and hence place greater uncertainty on the interpretation (Figure 12).

Strengths and limitations of paleoshoreline evaluations

The fossil record allows us to compare both paleoshorelines models, which lack adequate documentation of their input data, with paleobiological observations and give a semiquantitative measure of confidence for the paleoshoreline models. However, owing to spatio-

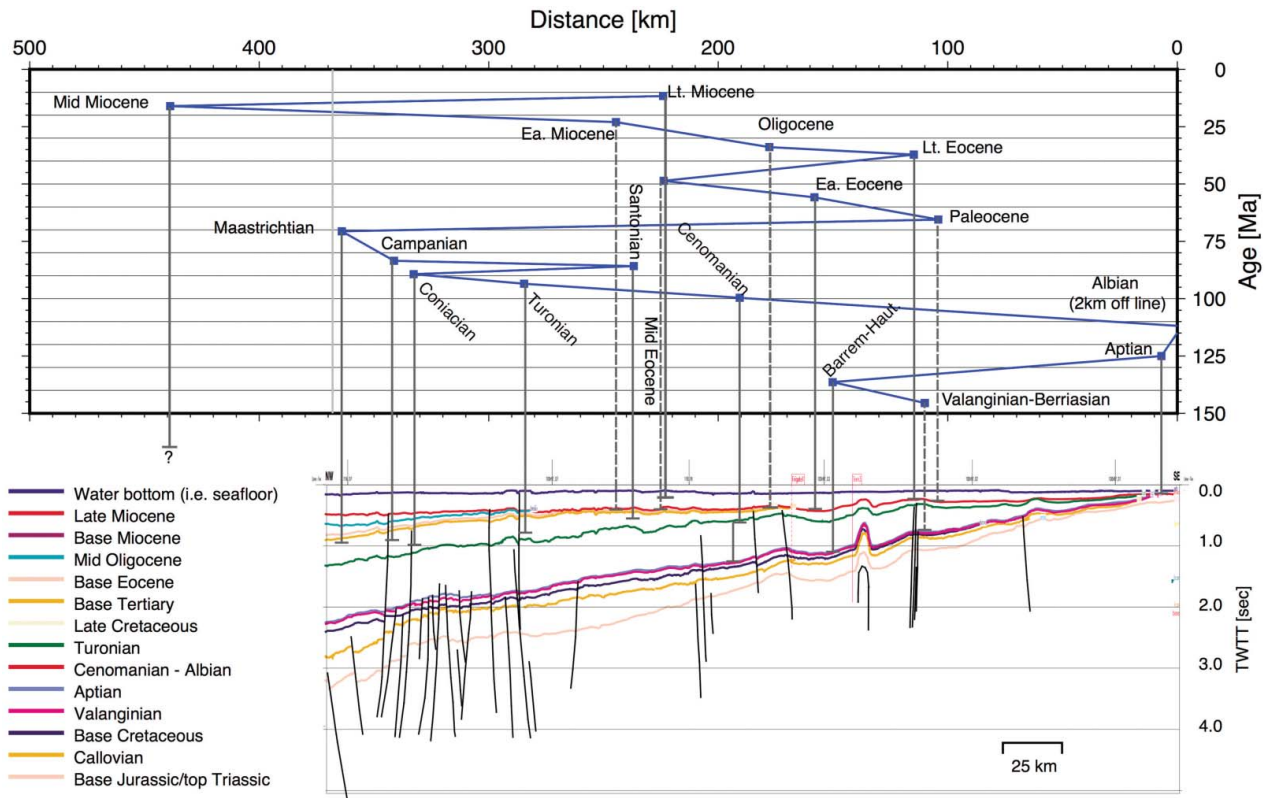


Figure 12 Synthetic paleoshoreline trajectories for AGSO Line 100/06 in the Bonaparte/Petrel basin based on Smith *et al.* (1994) and seismic horizon interpretation (Colwell & Kennard 2001). The upper part of the image shows the computed shoreline trajectory using geological time as depth (y axis) and using the shoreline intersection with the seismic profile as the x-location. Starting-point is the landward end of the seismic profile. Vertical lines with bars indicate the correlation between the x-position and the interpreted seismic horizon of the corresponding age interval. Solid vertical lines between the shoreline trajectory point (squares) and seismic horizon indicate that sufficient thickness exists to warrant that the shoreline could be identified on seismic data. Dashed vertical lines indicate a missing or very thin seismic horizon of corresponding age and hence a highly uncertain paleoshoreline positioning.

temporally heterogeneous sampling of the fossil record, the evaluation of time slices of the paleoshoreline models is biased. The consistency ratios of the paleoshorelines with the fossil record increase from the Cretaceous into the Cenozoic (Figure 9), likely related to an increase in the preservation potential of the geological record with progressively younger ages.

On a basin scale, as well as fossils, geological features within sedimentary formations, may also be used to evaluate paleoshoreline positions. For example, the Hooray Sandstone in the Eromanga Basin indicates fluvial to shallow marine conditions in the Berriasian to lower Aptian (Exon & Senior 1976; Senior *et al.* 1978), while the Doncaster Mudstone in the Surat Basin indicates marine flooding in the upper Aptian (Exon 1976; Exon & Senior 1976).

Methods not used in the creation of the paleogeographic maps may also be useful in the evaluation of paleogeographic evolution. Thermochronology from apatite fission track data (e.g. in southeastern Australia; Moore *et al.* 1986), the reflectivity of the coal maceral (vitrinite), and paleomagnetic indicators from magnetite and hematite (e.g. in the Sydney Basin; Middleton & Schmidt 1982) are commonly used as proxies for basin burial history for petroleum exploration. As

evolution of paleogeography is tied to drainage changes related to burial history, paleogeographic trends may be cross-checked with vertical elevation change trends derived from thermochronology.

The coverages of fossils, sediment outcrops, coal, magnetite, hematite and apatite are limited (see above; Middleton & Schmidt 1982; Moore *et al.* 1986). However, the combined usage of consistency measurements utilising data from these sources provides optimum data coverage. Evaluation of paleogeographic data using these techniques may be utilised on paleogeographic maps derived from older maps or without outcrop/well/seismic locations used in the interpretations plotted.

Our approach of constructing synthetic paleoshoreline trajectory plots and validating them with existing seismic data or seismic horizon interpretations offers a powerful method to locally evaluate the robustness of paleoshoreline data and will act as a starting-point for revised, and updated, paleoshoreline models.

CONCLUSIONS

Regional to global paleoshoreline analysis over geological time is a valuable tool to detect changes in

continental base level and hence provides powerful observational constraints for continental-scale dynamic topography models (e.g. Heine *et al.* 2010)

Global Cretaceous and Cenozoic flooding histories derived from the Smith *et al.* (1994) and Golonka *et al.* (2006) paleogeographic map sets largely agree with published eustatic trends. The Cenozoic flooding histories for both atlases is similar, while there are substantial differences in the first half of the Early Cretaceous and in the mid Cretaceous. Smith *et al.* (1994) predict greater flooding during these times, which corresponds with paleo-environments interpreted from fossil locations in the Early Cretaceous but not in the mid Cretaceous. We attribute the differences between the two atlases during these times to sampling protocols as well as to differences in the amount of smaller plates used for complex tectonic domains such as the western Tethys. The Australian flooding histories of Smith *et al.* (1994) and Golonka *et al.* (2006) are generally similar.

Consistencies between the land and flooding extents of both paleogeographic models with fossil locations are high with ratios upwards of 90%, despite major inconsistencies between the paleogeographic land extents with fossil data in Europe, Australia and North America in some time intervals. However, it should be noted that the greatest concentrations of fossils extracted from the Paleobiology Database and used in our analysis are also from these regions. This also corresponds to the level of sampling and the preservation potential of the individual regions. While similar comparisons between Smith *et al.* (1994), Golonka *et al.* (2006) and the Paleogeographic Atlas of Australia (Langford *et al.* 1995; Yeung 2002) in Cretaceous and Cenozoic Australia suggests very little overall difference in paleoshoreline–fossil consistency, minor variations do affect future studies on these datasets. Smith *et al.* (1994) has the highest consistency with fossil data in the Cretaceous, while the Upper Cretaceous–Cenozoic paleogeographic interpretations for all models may have to be reviewed in light of the fossil data from the Paleobiology Database.

Additional evaluation of seismic data from marginal basins together with paleoshoreline trajectory plots offers a quick way to assess the confidence in paleoshoreline interpretations.

The data sets analysed in this paper will provide a useful basis for testing geodynamic model predictions of regional dynamic topography through time against mapped flooding patterns. The digital compilation of global shoreline models is available as electronic supplement to this paper. Please check the GitHub repository (https://github.com/chhei/Heine_AJES_15_GlobalPaleoshorelines) or the EarthByte website (<http://www.earthbyte.org>) for a “live” version of the data.

ACKNOWLEDGEMENTS

We acknowledge Jan Golonka for making his global paleogeographic maps available to us. Work presented in this paper forms part of LY's dissertation at USYD. C. Heine was funded by ARC Linkage Project LP0989312 with Shell E&P, and TOTAL. R. D. Müller is supported by Australian Research Council grant FL0992245. We

gratefully acknowledge the reviews by Marita Bradshaw and Phil Schmidt.

SUPPLEMENTARY PAPERS

The digital compilation of global shoreline models is available as electronic supplement to this paper. Please check the GitHub repository (https://github.com/chhei/Heine_AJES_15_GlobalPaleoshorelines) or the EarthByte website (<http://www.earthbyte.org>) for a “live” version of the data.

REFERENCES

- BLAKEY R. 2003. Carboniferous–Permian global paleogeography of the assembly of Pangaea. In: *Symposium on Global Correlations and Their Implications for the Assembly of Pangea, Utrecht (August 10–16, 2003), International Congress on Carboniferous and Permian Stratigraphy*, p. 57. International Commission on Stratigraphy.
- BLAKEY R. C. 2008. Gondwana paleogeography from assembly to breakup 500 my odyssey. In: Fielding C. R., Frank T. D. & Isabell L. eds. *Resolving the late Paleozoic ice age in time and space*, pp. 1–28. Special Paper Geological Society of America 441, Boulder Co.
- BLAKEY R. C. & GUBITOSA R. 1984. Controls of sandstone body geometry and architecture in the Chinle Formation (Upper Triassic), Colorado Plateau. *Sedimentary Geology* 38, 51–86, doi: 10.1016/0037-0738(84)90074-5.
- BMR PALEOGEOGRAPHIC GROUP. 1990. *Australia: Evolution of a Continent. Bureau of Mineral Resources, Geology & Geophysics, Canberra, A.C.T., Australia.* http://www.ga.gov.au/corporate_data/22137/22137.pdf (accessed 2015-01-26).
- BOND G. 1976. Evidence for continental subsidence in North America during the Late Cretaceous global submergence. *Geology* 4, 557–560.
- BOYDEN J. A., MÜLLER R. D., GURNIS M., TORSVIK T. H., CLARK J. A., TURNER M., IVEY-LAW H., WATSON R. J. & CANNON J. S. 2011. Next-generation plate-tectonic reconstructions using GPlates. In: Keller G. R. & Baru C. eds. *Geoinformatics: Cyberinfrastructure for the Solid Earth Sciences*, pp.95–114. Cambridge University Press, Cambridge UK.
- CAMBRIDGE PALEOMAP SERVICES. 1993. *ATLAS version 3.3.* Cambridge Paleomap Services, P.O. Box 246, Cambridge, UK.
- COLWELL J. & KENNARD J. M. 2001. *Line Drawings of Interpreted Regional Seismic Profiles*, Offshore Northern and Northwestern Australia, URL http://www.ga.gov.au/metadata-gateway/meta_data/record/36353/. Canberra ACT.
- EXON N. F. 1976. *Geology of the Surat Basin in Queensland*, vol. 166, Australian Government Publishing Service, Canberra ACT.
- EXON N. & SENIOR B. 1976. The Cretaceous of the Eromanga and Surat Basins. *BMR Journal of Australian Geology and Geophysics* 1, 33–50.
- GOLONKA J., KROBICKI M., PAJAK J., VAN GIANG N. & ZUCHEWICZ W. 2006. *Global Plate Tectonics and Paleogeography of Southeast Asia*, Faculty of Geology, Geophysics and Environmental Protection, AGH University of Science and Technology, Arkadia, Krakow, Poland.
- GRADSTEIN F. M., OGG J. G. & SMITH A. G. 2004. *A geologic time scale 2004*, vol. 86. Cambridge University Press, Cambridge UK.
- GURNIS M. 1990. Bounds on global dynamic topography from Phanerozoic flooding of continental platforms. *Nature* 344, 754–756, doi: 10.1038/344754a0.
- GURNIS M. 1993. Phanerozoic marine inundation of continents driven by dynamic topography above subducting slabs. *Nature* 364, 589–593.
- GURNIS M., MÜLLER R. & MORESI L. 1998. Cretaceous vertical motion of Australia and the Australian Antarctic discordance. *Science* 279, 1499–1504, 10.1126/science.279.5356.1499.
- HAHN L. 1982. The Triassic in Thailand. *Geologische Rundschau* 71, 1041–1056, doi: 10.1007/BF01821117,10.1007/BF01821117.
- HAQ B. U. & AL-QAHTANI A. M. 2005. Phanerozoic cycles of sea-level change on the Arabian Platform, *GeoArabia* 10, 127–160.
- HARLAND W. 1990. *A Geologic Time Scale 1989*, Cambridge University Press, Cambridge, United Kingdom.

- HAY W., DECONTO R., WOLD C., WILSON K., VOIGT S., SCHULZ M., WOLD A., DULLO W., RONOV A., BALUKHOVSKY A. & SODING E. 1999. Alternative global Cretaceous paleogeography. *In*: Barrera E. & Johnson C. eds. *Evolution of the Cretaceous ocean/climate system*, pp. 1–47. Geological Society of America Special Paper 332, Boulder Co. doi: 10.1130/0-81372332-9.1.
- HEINE C., MÜLLER R., STEINBERGER B. & DiCAPRIO L. 2010. Integrating deep Earth dynamics in paleogeographic reconstructions of Australia. *Tectonophysics* **483**, 135–150, doi: 10.1016/j.tecto.2009.08.028, 2010.
- KISSLING W. & FLÜGEL E. 2000. Late Paleozoic and Late Triassic limestones from North Palawan Block (Philippines): Microfacies and paleogeographical implications. *Facies* **43**, 39–77, doi: 10.1007/BF02536984.
- KISSLING W., FLÜGEL E. & GOLONKA J. 1999. Paleoreef maps: Evaluation of a comprehensive database on Phanerozoic reefs. *AAPG Bulletin* **83**, 1552–1587.
- KISSLING W., FLÜGEL E. & GOLONKA J. 2003. Patterns of Phanerozoic carbonate platform sedimentation. *Lethaia* **36**, 195–225, doi: 10.1080/00241160310004648.
- LANGFORD R., WILFORD G., TRUSWELL E. M. & ISERN A. R. eds. 1995. *Paleogeographic atlas of Australia*, Australian Geological Survey Organization, Canberra, ACT. ISBN 0 644 13005 9.
- MASSON D. G. & ROBERTS D. G. 1981. Late Jurassic–Early Cretaceous reef trends on the continental margin SW of the British Isles. *Journal of the Geological Society* **138**, 437–433, doi:10.1144/gsjgs.138.4.0437.
- MATTHEWS K. J., HALE A. J., GURNIS M., MÜLLER R. D. & DiCAPRIO L. 2011. Dynamic subsidence of eastern Australia during the Cretaceous. *Gondwana Research* **19**, 372–383.
- MIDDLETON M. & SCHMIDT P. 1982. Paleothermometry of the Sydney basin. *Journal of Geophysical Research: Solid Earth* (1978–2012) **87**, 5351–5359.
- MOORE M. E., GLEADOW A. J. & LOVERING J. F. 1986. Thermal evolution of rifted continental margins: new evidence from fission tracks in basement apatites from southeastern Australia. *Earth and Planetary Science Letters* **78**, 255–270.
- MÜLLER R., SDROLIAS M., GAINA C., STEINBERGER B. & HEINE C. 2008. Long-term sea-level fluctuations driven by ocean basin dynamics. *Science* **319**, 1357–1362, doi: 10.1126/science.1151540.
- PETTERS S. 1979. Stratigraphic history of the south-central Saharan region. *Bulletin of the Geological Society of America* **90**, 753–760, doi: 10.1130/0016-7606(1979)90<753:CO>2.
- RONOV A., KHAIN V. & BALUKHOVSKY A. 1989. *Atlas of lithological-paleogeographical maps of the world: Mesozoic and Cenozoic of continents and oceans*, USSR Academy of Sciences, Moscow, Union of Soviet Socialist Republics.
- SCOTSE C. 2004. A continental drift flipbook. *The Journal of Geology* **112**, 729–741, doi: 10.1086/424867.
- SENIOR B., MOND A. & HARRISON P. 1978. *Geology of the Eromanga Basin*, Australian Government Publishing Service, Canberra ACT.
- SLOSS L. 1988. Tectonic evolution of the craton in Phanerozoic time. *The Geology of North America* **2**, 25–51.
- SMITH A., SMITH D. G. & FURNELL B. M. 1994. *Atlas of Mesozoic and Cenozoic coastlines*, Cambridge University Press, Cambridge, United Kingdom, 112 p.
- SPASOJEVIC S. & GURNIS M. 2012. Sea level and vertical motion of continents from dynamic earth models since the Late Cretaceous. *AAPG Bulletin* **96**, 2037–2064.
- USGS. 2011. *World Geologic Maps*, United States Geological Survey Energy Resources Program, Reston, Virginia, United States.
- VEEVERS J. 1969. Palaeogeography of the Timor Sea Region. *Palaeogeography, Palaeoclimatology, Palaeoecology* **6**, 125–140, doi: 10.1016/0031-0182(69)90008-X.
- VEEVERS J. & MORGAN P. 2000. *Billion-year Earth history of Australia and neighbours in Gondwanaland*, GEMOC Press, Sydney, Australia.
- WINTERER E. 1991. The Tethyan Pacific during Late Jurassic and Cretaceous times. *Palaeogeography, Palaeoclimatology, Palaeoecology* **87**, 253–265, doi: 10.1016/0031-0182(91)90138-H.
- YEUNG M. 2002. *Palaeogeographic atlas of Australia*, Geoscience Australia, Canberra ACT.
- ZIEGLER M. A. 2001. Late Permian to Holocene Paleofacies Evolution of the Arabian Plate and its Hydrocarbon Occurrences. *GeoArabia* **6**, 445–504, <http://www.searchanddiscovery.com/documents/ziegler/images/ziegler.pdf>.

Received 12 December 2013; accepted 22 December 2014